

Metastability and uniqueness of vortex states at depinning

Mahesh Chandran, R. T. Scalettar, and G. T. Zimányi

Department of Physics, University of California, Davis, California 95616

(Dated: December 2, 2024)

We present results from numerical simulations of transport of vortices in the zero-field cooled (ZFC) and the field-cooled (FC) state of a type-II superconductor. In the absence of an applied current I , we find that the FC state has a lower defect density than the ZFC state, and is stable against thermal cycling. On the other hand, by cycling I , surprisingly we find that the ZFC state is the stable state. The FC state is metastable as manifested by increasing I to the depinning current I_c , in which case the FC state evolves into the ZFC state. We also find that the configuration of moving vortices has a unique defect density independent of the method of preparation at the depinning transition.

PACS numbers: 74.60.Ge, 74.60.Jg

Metastability is a generic feature in many disordered systems. Metastable states show characteristics distinct from the ground state, and are evidenced, for example, by the path or history dependence of the different response functions. A striking example of metastability is the difference between the field-cooled (FC) and zero-field cooled (ZFC) magnetisation and susceptibility in vortex phase of type-II superconductors[1]. In superconductors, the FC magnetisation is much smaller than the ZFC magnetisation. This difference decreases with increasing temperature and vanishes above the irreversibility temperature T_{irr} . The ZFC state is believed to be metastable and the FC state to be an equilibrium state, because it is possible to reach the FC state from the ZFC state by changing T from a low value to T_{irr} and back, but the ZFC state cannot be reached from a FC state through such a temperature cycle. Similar features are also observed in spin glasses [2]. The difference in FC and ZFC state magnetisation is explained by the emergence of energy barriers for $T < T_{irr}$, which increase with decreasing T . In certain models like the vortex glass, the energy barrier is believed to diverge at a temperature $T_g \leq T_{irr}$ [3, 4], which can lead to infinitely long-lived metastable states.

In the anomalous peak effect region the situation is reversed: the FC state has been shown to be unstable against current annealing. The critical current I_c is higher in the virgin FC state than in FC states annealed by a current or in the ZFC state [5, 6]. Also, the susceptibility of the FC state can be switched to that of the ZFC state by applying an ac pulse [7]. Moreover, recent scanning Hall probe measurements have shown substantial vortex rearrangement in FC states for $I < I_c$ [8]. One approach accounts for these experimental observations through the role of surface barriers [9]. These differing pictures place in the focus the behavior of vortices in the FC and ZFC state in the presence of a transport current.

In this paper we use numerical simulations to study the transport of differently prepared vortex systems. Our first main result is that, in contrast to the temperature

cycling, if the vortex system is cycled with a transport current, then the ZFC state is more stable than the FC state. In particular, the ZFC state can be reached from the FC state by current cycling, but not vice versa. Our second main result is that, with increasing currents, all vortex states, FC, ZFC, or prepared in any intermediate way, acquire the same *density of defects at depinning*, a type of universality for plastic depinning.

We consider vortices in a 2D plane perpendicular to the magnetic field $\mathbf{B} = B\hat{\mathbf{z}}$ of a bulk superconductor, with $B = n_v\phi_0$ where n_v is the vortex density, and ϕ_0 is the flux quantum. Within the London approximation we treat the vortices as particles, with dynamics governed by an overdamped equation of motion,

$$\eta \frac{d\mathbf{r}_i}{dt} = - \sum_{j \neq i} \nabla U^v(\mathbf{r}_i - \mathbf{r}_j) - \sum_k \nabla U^p(\mathbf{r}_i - \mathbf{R}_k) + \mathbf{F}_{ext} + \zeta_i(t).$$

Here η is the flux-flow viscosity, and the first term represents the inter-vortex interaction given by the potential $U^v(r) = \frac{\phi_0}{8\pi^2\lambda^2} K_0(\tilde{r}/\lambda)$, where K_0 is the zero-order Bessel function, and $\tilde{r} = (r^2 + 2\xi^2)^{1/2}$ with λ and ξ as penetration depth and coherence length of the superconductor, respectively [10]. The second term is the attractive interaction with parabolic potential wells $U^p(r) = U_0(\frac{r^2}{r_p^2} - 1)$ for $r < r_p$, and 0 otherwise, centered at the random \mathbf{R}_k locations. The third term $\mathbf{F}_{ext} = \frac{1}{c}\mathbf{J} \times \phi_0\hat{\mathbf{z}}$ represents the Lorentz force due to the transport current density \mathbf{J} . The last term is the thermal noise (Langevin term) with the moments $\langle \zeta_{i,p}(t) \rangle = 0$, and $\langle \zeta_{i,p}(t)\zeta_{j,p'}(t') \rangle = 2k_B T \eta \delta_{ij} \delta_{pp'} \delta(t - t')$, where T is the temperature, k_B is Boltzmann constant, and $p, p' = x, y$. We worked with reduced variables: the current density J in units of cf_0/ϕ_0 , and T in units of $\lambda_0 f_0/k_B$, where $\lambda(T = 0) = \lambda_0$, and $f_0 = \frac{\phi_0}{8\pi^2\lambda_0^3}$. This model is expected to reasonably capture the physics of stiff vortex lines, like those in Nb , $NbSe_2$, and so on, while in strongly layered superconductors, as in the cuprates, the soft interlayer couplings introduce additional degrees of freedom.

To simulate the ZFC state, we confine the quenched disorder to a central region of the simulation box, while leaving the outer region defect free as illustrated in Fig. 1. The disordered region defines the extent of the superconductor and the disorder free region simulates the free-space. Periodic boundary conditions connect the edges of the simulation box. We employ a box of size $40\lambda_0 \times 24\lambda_0$, with the disordered region occupying $28\lambda_0 \times 24\lambda_0$. We used a pin density of 5.95 per unit area with an average $U_0 = 0.03$, and $r_p = 0.1\lambda_0$. The results presented below are for $N_v = 1148$ vortices in the simulation box which corresponds to $B \approx 800G$. The real space defect density in the vortex configuration is obtained by Delaunay triangulation. The $V(I)$ characteristics are calculated by varying $\mathbf{F}_{ext} = F_{ext}\hat{\mathbf{x}}$ ($F_{ext} \propto I$, the current) and calculating the average velocity ($\propto V$, the voltage) $\mathbf{v} = \frac{1}{N_v} \sum_i^{N_v} \dot{\mathbf{r}}_i$ along the x -axis.

We first consider the effect of cycling the temperature T . The ZFC state at $T = 0$ is created by positioning vortices in the defect free region and allowing them to move into the disordered region by their own dynamics. The FC state is created by the thermal cycle starting in the ZFC state at $T = 0$, then heating the system deep into the liquid phase, and subsequently cooling it back to $T = 0$. Fig. 1 shows the behaviour of the defect density n_d throughout this thermal cycle. Since the ZFC state at $T = 0$ is formed by vortices diffusing into the disordered region, this leads to a gradient in vortex density [11], explaining the large defect density in the ZFC state. Across $T = 0.012 = T_m$, the melting temperature, $n_d(T)$ rapidly increases to higher values, as the system goes into the liquid phase. Compared to the ZFC state, the FC state has a lower $n_d(0)$ at $T = 0$ as it is cooled from the homogeneous liquid phase that has no macroscopic density gradients. The FC state shows no appreciable change in n_d on repeated thermal cycling. The inset in Fig. 1 shows the hysteresis in n_d on crossing T_m , which is evidence for the melting transition into the liquid phase being first order. A very slow cooling rate is used in the inset, compared to the main panel, to more accurately observe the hysteresis across T_m .

A partial thermal cycling of the system, consisting of a warming step to a temperature T_{PFC} , e.g. $T_{PFC} = 0.006 = \frac{T_m}{2}$, and a subsequent cooling step to $T = 0$ (see Fig. 1) generates a partially field-cooled (PFC) state. The PFC state is less disordered than the ZFC state, and is stable to thermal cycling between 0 and T_{PFC} . For $T > T_{PFC}$, the PFC state follows the same path as the virgin ZFC state, a phenomenon that can be named partial stability. This repeated warming and cooling allows one to access all the other PFC configurations at $T = 0$. The behaviour of $n_d(T)$ is in consonance with the experimental measurement of magnetisation $M(T)$, which shows similar behaviour below T_{irr} [1].

Next we consider the effect of a transport current I on various configurations. As shown in Ref.[12], the effects

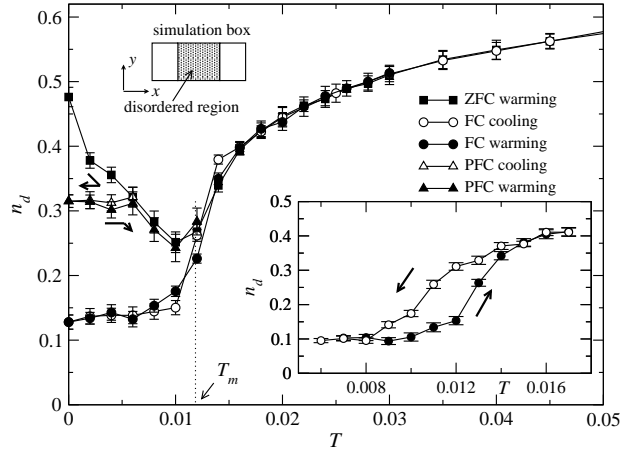


FIG. 1: Plot of $n_d(T)$ for the thermal cycling starting with the ZFC state at $T = 0$. Also shown is the partial stability of the PFC state, created by cooling from $T_{PFC} = 0.006$. The direction in which T is changed for creating the PFC state is shown by thick arrows. The simulation geometry is shown on the upper left corner of the main panel. Inset : hysteresis in n_d across T_m during the FC cooling and warming procedure.

of the disorder can be characterized by an effective “shaking temperature” T_{sh} . $T_{sh} \propto v^{-1}$, where $v \propto I$ is the vortex velocity, implying that at large currents the effect of disorder is small, and the vortex system recrystallizes. Therefore, besides the above described thermal cycling, the disordered vortex state can be prepared by current cycling as well. In particular, starting with a flowing vortex lattice at large enough currents, a disordered vortex state is formed by reducing I to zero across the depinning current I_c . As will be shown below, the resulting configuration is the most stable vortex state against repeated cycling of I . We call the resulting static configuration the current hardened (CH) state, in analogy to “strain hardening”, in which materials are cycled with increasing stress to increase the density of dislocations.

Fig. 2 shows $V(I)$ and $n_d(I)$ curves at $T = 0$ for differently prepared states. We identify three current regimes : (1) a pinned regime $I < I_c$, with $V = 0$ and $n_d(I)$ determined by the mode of preparation; (2) a plastic regime $I_c < I < I_m$, with non-linear $V(I)$ and the same $n_d(I)$ for all differently prepared states; and (3) a flowing-lattice regime $I > I_m$, with linear $V(I)$ and $n_d(I)$ substantially smaller. The small difference in n_d in the flowing-lattice regime, as seen in Fig. 2, is due to the formation of a grain boundary at the free edges of the disorder region (see also Fig. 4(c)). Remarkably, $V(I)$ curves and the depinning current I_c are independent of the mode of preparation of the system. These characteristics persist at finite T as well. The $n_d(I)$ for $I < I_c$, on the other hand, depends on the mode of preparation.

Strikingly, the defect density $n_d(I)$ at the depinning current I_c assumes the same value $n_d^c \approx 0.51$ for the FC, ZFC, PFC, and CH states, as seen in Fig. 2. In other

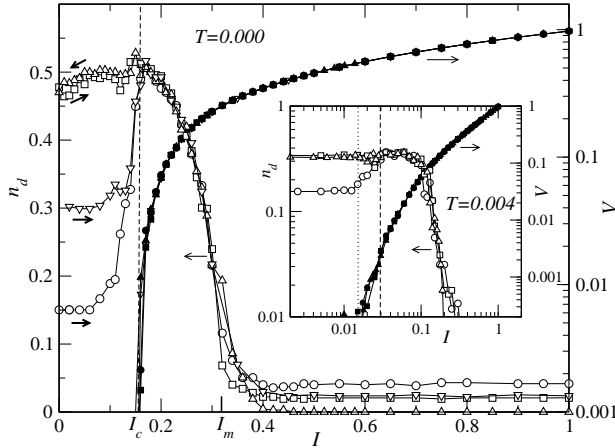


FIG. 2: $V(I)$ (filled symbols), and $n_d(I)$ (open symbols) at $T = 0$ for the FC state (\circ), PFC state (∇), ZFC state (\square), and CH state (\diamond). The direction in which current is changed is shown by thick arrows. Inset : same as the main panel for $T = 0.004$. The dashed and the dotted lines mark I_{irr} and I_c , respectively.

words, n_d^c is *independent of the mode of the preparation of the vortex state*. The preparation independent, “universal” value of n_d^c implies that the characteristics and dynamics of all vortex states converge as the current approaches I_c . This idea is substantiated by studying the dynamics of the vortex system at the depinning directly. As is known, vortices depin by forming a few transport channels across the system [13]. We find that, while in differently prepared states the channels are nucleated at different locations along the entry edge, in the bulk the channels converge quickly to a universal pattern. We also find the average transverse wandering of a channel is of the order of ~ 6 -7 lattice constants, and is same for all states at I_c . This implies that the average displacement of the vortices at I_c is the same for all states, thus providing an underlying physical picture for preparation independence of n_d^c . Further studies show that the value of n_d^c depends on T , n_v , and the disorder strength.

Next, we study the stability of the different vortex states against cycling with currents. At zero current the virgin FC state has a defect density of $n_{d,FC}(0) < n_d^c$. Therefore, the density of defects in the virgin FC state has to increase from $n_{d,FC}(0)$ to n_d^c as the current is increased from 0 to I_c . As shown in Fig. 2, $n_{d,FC}(I)$ indeed grows with increasing currents for $I < I_c$. Furthermore, decreasing current from $I_1 < I_c$, $n_{d,FC}(I)$ does not decrease to its virgin value, but stays approximately at $n_d(I_1)$. In particular, cycling I between 0 and $I \geq I_c$ leaves $n_{d,FC}(I) \approx n_d^c$ for $I < I_c$. At the same time, $n_{d,ZFC}(0) \approx n_d^c$, and cycling I does not affect this value. Therefore, the FC state, and its defect density $n_{d,FC}$, can be transformed into the ZFC state and $n_{d,ZFC}$ by cycling I between 0 and I_c . The reverse is not true, *i.e.*, the FC state cannot be reached from any state by cycling

current. Therefore, in contrast to thermal cycling, we find that the FC state is metastable and the ZFC state is stable against current cycling. Fig. 2 further illustrates that the current hardened state and its defect density $n_{d,CH}(I)$ evolve into the ZFC state when the current is decreased from a large value to 0. The same holds for the PFC states, as $n_{d,PFC}(I)$ also evolves into $n_{d,ZFC}(0)$.

Previous studies of elastic models have reported the presence of metastable states below I_c and the uniqueness of the moving phase at the depinning transition [14]. These models neglect topological defects, *e.g.*, phase slips in 1-d, and dislocations in 2-d. In contrast, the depinning transition at I_c in our simulation is through plastic deformations of the system, which induce a high density of dislocations. Remarkably, in spite of the presence of dislocations, we observe metastable states and universal features of the dynamics at I_c , such as the defect density n_d^c . We also find that the differently prepared vortex states develop an approximately unique configuration at I_c , in analogy with the elastic model.

Since for $I > I_c$ $n_d(I)$ is approximately the same for all states, metastable configurations and the irreversible behavior of $n_d(I)$ emerge only below I_{irr} . For $T = 0$, $I_{irr} = I_c$, but at finite temperatures these two current values separate, as evident for $T = 0.004$, shown in the inset of Fig. 2. At finite T , $n_d(I) \approx n_d^c$ at a current $I_{irr} > I_c$. This is possibly due to thermally activated vortex creep, which induces vortex displacements already for $I < I_{irr}$. The metastability of the FC state persists at finite T , and we believe is a generic phenomenon which brings out a fundamental difference in the nature of FC and ZFC states. The ZFC and CH states show similar behavior throughout the studied current and temperature ranges.

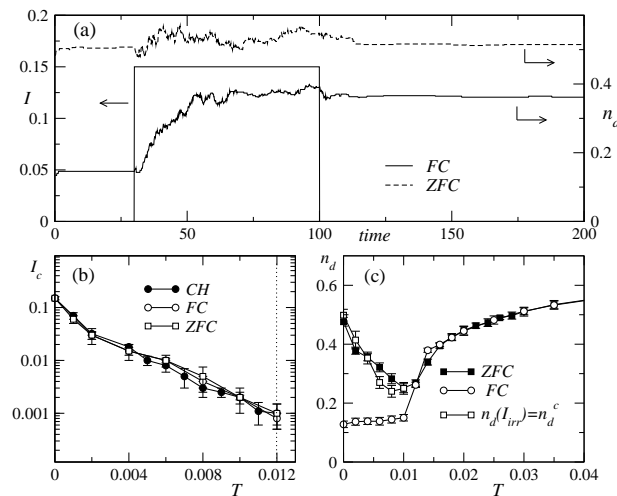


FIG. 3: (a) The time evolution of n_d at $T = 0.0$ for a pulse of current $I = 0.15 < I_c$ in the ZFC and the FC state. (b) Plot of $I_c(T)$ obtained from FC, ZFC and CH states. (c) Shows $n_d^c(T)$ obtained from $V(I)$ curves along with n_d for ZFC warming and FC cooling superimposed from Fig. 1.

Further evidence for metastability of the FC state is

obtained by applying a current pulse $I = 0.15 < I_c$ to differently prepared vortex states, and observing the temporal evolution of n_d , as illustrated in Fig. 3(a). The application of a current pulse evolves the FC state into PFC states with an intermediate defect density $n_{d,FC} < n_{d,PFC} < n_{d,ZFC}$. The defect density remains at that elevated level even after the current drops to zero. In particular, a large enough current pulse evolves the FC state into the ZFC state. This transformation of the FC state to the ZFC state by a current pulse is in close analogy to experimental observations [7]. We emphasize that the transformation of the FC state to ZFC state as found here is a bulk characteristic. This is unlike Ref.[7] which finds a change in I_c during the transformation, possibly due to the influence of surface barrier [15].

In Fig. 3(b) we plot $I_c(T)$ for a range of T at which simulations were carried out. The I_c follows an $\exp(-\frac{T}{T_0})$ form, confirming that thermally activated motion dominates the dynamics at I_c . Fig. 3(c) shows the temperature dependence of $n_d^c(T)$, as obtained from $V(I)$ curves. The $n_d(T)$ values for the FC and ZFC states are superimposed from Fig. 1. $n_d^c(T)$ closely follows $n_{d,ZFC}(T)$, obtained by warming the ZFC state, thus corroborating the view that the ZFC state is essentially the frozen equivalent of the critical state at I_c .

The configurational changes are illustrated in Fig. 4 for various states, during a composite T - I cycle. Starting with the ZFC state, shown in Fig. 4(a), we obtain the FC state (Fig. 4(b)) by cycling T from 0 to $T > T_m$. The FC state is then driven with $I > I_m$ to obtain Fig. 4(c). And finally, decreasing I to 0, the CH state is obtained in Fig. 4(d), which is indistinguishable from the ZFC state in Fig. 4(a). *Thus a composite T – I cycle allows one to go from the ZFC state to the FC state and vice-versa.* The ZFC state shows a dense network of dislocations, with the ordered region not extending beyond 2-3 lattice constants. On the other hand, the FC state shows relatively large ordered regions and defects are primarily bound dislocations, with a low density of unbound dislocations, as seen in Fig. 4(b). Applying currents $I > I_m$ further order the system, as shown in Fig. 4(c), where the lone grain boundary is due to the free boundaries of the disordered region. Finally, reducing I to 0 across I_c reintroduces large scale defects, leading to a configuration indistinguishable from the ZFC state.

In conclusion, we have shown that the ZFC state is stable against cycling current. In contrast, the FC state is found to be metastable against current cycling. This behavior is opposite to the thermal cycling, where the FC state is stable. The defect density n_d for any initial preparation converges to the same value n_d^c at I_c , showing a remarkable uniqueness of the moving phase at depinning.

We thank Helmut Katzgraber for critical reading of the manuscript. M.C. also acknowledges useful discussions with E. Zeldov and A. K. Grover during the course of the

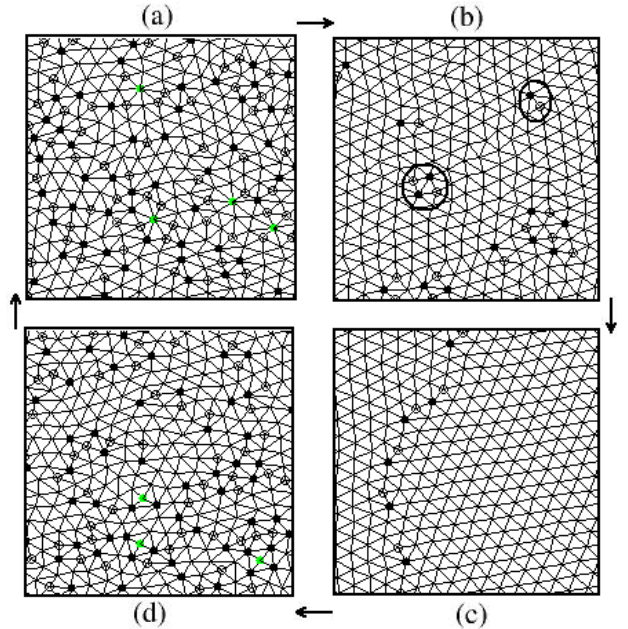


FIG. 4: The real space configuration at $T=0$ during a composite T - I cycle : (a) ZFC state, (b) FC state, (c) flowing lattice state, (d) CH state. The arrows show the cycling path (see text for details). Note the close similarity between (a) and (d). The symbols (o) and (●) denote vortices with 5 and 7 neighbours, respectively. A free dislocation, and a bound pair of dislocation are encircled in (c).

work. This work was supported by NSF-DMR 9985978.

- [1] K. A. Müller, M. Takashige, and J. G. Bednorz, Phys. Rev. Lett. **58**, 1143 (1987).
- [2] K. Binder, and A. P. Young, Rev. Mod. Phys. **58**, 801 (1986); K. H. Fischer, and J. A. Hertz, *Spin Glasses* Cambridge University, Cambridge, (1991).
- [3] D. S. Fisher, M. P. A. Fisher, and D. A. Huse, Phys. Rev. B **43**, 130 (1991).
- [4] G. Blatter *et al.*, Rev. Mod. Phys. **66**, 1125 (1994).
- [5] W. Henderson *et al.*, Phys. Rev. Lett. **77**, 2077 (1996).
- [6] Z. L. Xiao *et al.*, Phys. Rev. Lett. **85**, 3265 (2000).
- [7] S. S. Banerjee *et al.*, Appl. Phys. Lett. **74**, 126 (1999).
- [8] M. Marchevsky, M. J. Higgins, and S. Bhattacharya, Phys. Rev. Lett. **88**, 087002 (2002).
- [9] Y. Paltiel *et al.*, Nature **403**, 398 (2000).
- [10] J. R. Clem, J. Low Temp. Phys. **18**, 427 (1975).
- [11] C. P. Bean, Phys. Rev. Lett. **8**, 250 (1962). For low vortex density, it is possible to prepare a ZFC state with partial penetration of vortices into the superconductor. Here, we deal with ZFC states in which vortices have penetrated fully into the bulk of the superconductor.
- [12] A. E. Koshelev, and V. M. Vinokur, Phys. Rev. Lett. **73**, 3580 (1994).
- [13] Moon K., R. T. Scalettar, and G. T. Zimányi, Phys. Rev. Lett. **77**, 2778 (1996); N. Grønbech-Jensen, A. R. Bishop, and D. Domínguez, Phys. Rev. Lett. **76**, 2985 (1996); Seungoh Ryu *et al.*, Phys. Rev. Lett. **77**, 5114 (1996); C. J. Olson, C. Reichhardt, and F. Nori, Phys. Rev. Lett.

80, 2197 (1998); Hans Fangoehr, Simon J. Cox, and Peter A. J. de Groot Phys. Rev. B **64**, 064505 (2001).

[14] D. S. Fisher, Phys. Rev. Lett. **50**, 1486 (1983); Phys. Rev. B **31**, 1396 (1985); A. A. Middleton and D. S. Fisher, Phys. Rev. Lett. **66**, 92 (1991); P. Chauve, T. Giamarchi, and P. Le Doussal, Phys. Rev. B **62**, 6241 (2000).

[15] Z. L. Xiao *et al.*, Phys. Rev. B **65**, 094511 (2002).